Study on the Formability & Shape Conformity of Mg & Al-alloy sheets in Warm condition by Electromagnetic Forming

M. Singhal, P.P. Date

Department of Mechanical Engineering, Indian Institute of Technology, Bombay, India.

Abstract

Electromagnetic forming is a high strain rate process used for shaping metals. Mg-alloys are of interest by virtue of the light weight and potential for application in automotive industries. These alloys have poor formability at room temperature and have to be formed under warm working conditions. Simulations using COMSOL Multiphysics software were carried out to predict the forming behavior of Mg-alloy sheets deformed at high speeds and different temperatures into a die with a corrugated shape. Conformance of the sheet to the die shape is the objective of this study. These sheets are assumed to be externally heated to different temperatures prior to forming. Possible changes in the mechanical and electrical properties of the material with temperature have been incorporated to show their individual and combined effects. A virtual circuit was built to excite the coil, fully coupled with the Solid Mechanics & Magnetic Fields, through related physics in the software. Optimal parameters that ensure good conformance to die shape are sought as the outcome of the simulation of warm electromagnetic forming of magnesium & aluminium alloy sheets. The quality of strain distribution under different clamping constraints was assessed using the strain non-uniformity index (SNI).

Keywords

Warm electromagnetic forming, shape conformity, failure criteria

1 Introduction

Magnesium alloys, being the lightest structural material available, has great mass saving potential as compared to aluminium & plastics [1]. Its applications have been explored in various sectors of industry, viz., automobile, aerospace, consumer electronics etc. A high strength to weight ratio, good impact strength & castability etc. make it amenable to manufacturing though the alloys have limited ductility at room temperature [2]. Deformation of these alloys in warm conditions improves their ductility. Strain hardening,

grain growth, dynamic recovery (DRV) and dynamic recrystallization (DRX) together influence the mechanical properties. The activation of non-basal slip systems and DRX are the major contributing mechanisms leading to softening at elevated temperatures [3].

Ulacia et.al. [4] found experimentally that deformation in Al increases at high temperature with an increase in the discharge energy. At a given discharge energy, deformation was found to decrease with increasing temperature presumably due to a lower electrical conductivity of the material leading to a lower Lorentz force despite small softening of the material. In contrast, experimental research of Murakoshi et.al. [5] showed increasing deformation of Mg sheets with increasing temperature.

In the present study, simulation of deformation of two different materials, namely, Magnesium and Aluminium into a multi-impression die at two levels of discharge energies and temperatures were studied using the COMSOL software. Two end-constraints (viz., fully free, fully constrained) have been deployed to study their effect on the extent of cavity filling by the sheet. The geometry of deformation considered is shown in figure 1a and 1b. The coupling of three physics, viz., the virtual electrical circuit, corresponding Lorentz forces generated and the consequent plastic deformation is schematically shown in figure 2. The Cowper-Symonds (CS) model was used to characterize the constitutive equation for the Magnesium alloy (Table 1) and the Johnson-Cook model for Aluminium alloy (Table 2). In the present work, anisotropy has not been considered because at high temperature prismatic $\{10\bar{1}0\}$ $<11\bar{2}0>$ and pyramidal $\{10\bar{1}1\}$ $<11\bar{2}0>$ slip planes get activated and hence the observed improvement in formability and reduction in anisotropy [6]. The high strain rate deformation occurring in the electromagnetic forming process converts 90-95% of the plastic work to heat. Since process time is very small (~50 µsec), this small adiabatic heating adds to the thermal softening. In the present study, this adiabatic thermal softening is neglected. The optimum factor level settings for maximum cavity filling and minimum non-uniformity in strain distribution over the deforming sheet are the expected outcomes of the study.

2 Simulation Procedure

2.1 Die-Sheet Configuration

The 3D setup of die, sheet and coils is realized in 2D axisymmetric mode (figure 1). The die considered has 4 regular cavities with a die entry radius of 6mm and die cavity width of 12 mm. The sheet thickness is 1 mm for all the simulations. The copper coil considered has a rectangular section (8 mm x 10 mm) with a radius of 2 mm at all the corners. Each turn is aligned with the centre of each cavity to maximise cavity filling. All gaps between elements of the configuration are assumed to be filled with ambient air.

2.2 Numerical Model

COMSOL Multiphysics is used in the present study as a numerical analysis tool which couples all the physics involved (viz., Virtual Circuitry, Electromagnetics, Solid Mechanics and Thermal Strains).

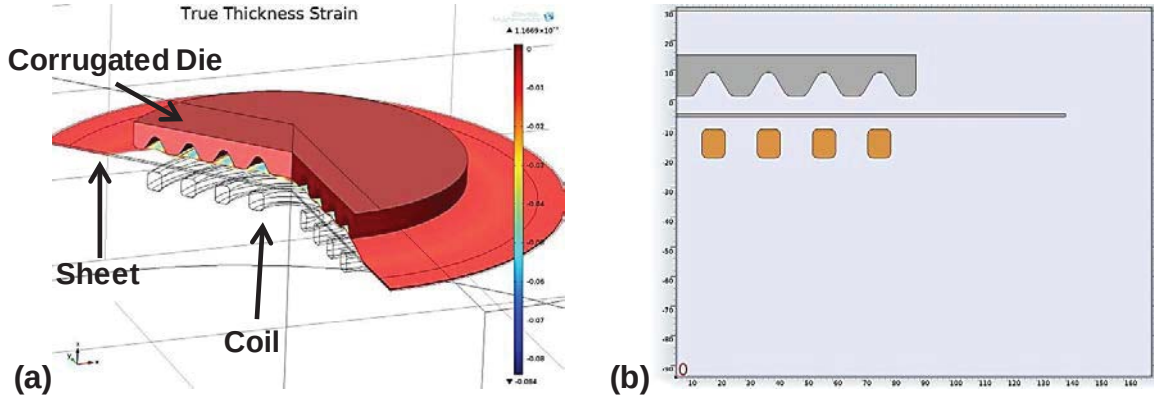

Figure 1: *(a) 3D Configuration, (b) 2D axisymmetric configuration*

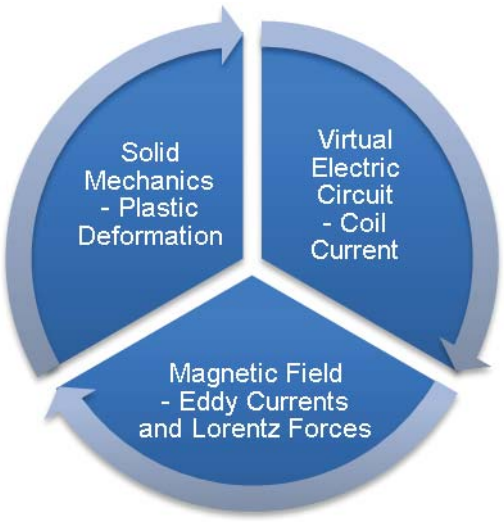

Figure 2*: Simulation Configuration (Coupling of multiple physics)*

Present configuration consists of a virtual circuit made by connecting each turn of the copper coil in series by means of nodes. Each turn (out of 4 turns) of the coil is labelled as a separate coil domain, and these domains are now connected to a virtual circuit in series by means of terminals. Now a capacitor with fixed capacitance and some initial charge (voltage) is also connected in series along with some resistance. This circuit is based on fundamental Kirchhoff's laws and hence takes the form of a ringing R-L-C Circuit. The resistance of the exciting circuit is considered to be a part of this circuit while the resistive losses of the coil-sheet system are considered separately. Now these currents are fed to the Magnetic field interface through a coupling variable. Magnetic field physics consists of air (insulator), coil and sheet. It solves for strong transient magnetic field generated in the vicinity of coil and hence current density induced in the electromagnetically connected sheet. The electromagnetic forces calculated on the sheet by means of the Maxwell stress tensor are inserted as body loads into the Solid Mechanics interface. Hence deformation in the sheet is achieved. Here, die is assumed to be completely rigid. Rayleigh damping, which provides mass damping and stiffness damping parameters, is used.

COMSOL uses penalty method approach to model contact between the sheet and the die [7]. Suitable penalty factor settings for contact are very important as inappropriate values may lead to ill-conditioned Jacobian matrix and convergence problems. To include friction in the contacts, static coulomb friction model was used. A constant value of 0.05 is assumed for static friction coefficient in the present case. As the sheet is assumed to have an initial temperature, thermal strains are also calculated. The sheet is being analysed for two different end constraints. In first case, sheet is set fully free, in second case, its end is fully constrained.

The present study is based on two materials, namely, 1 mm thick sheet of commercial AZ31B-H24 magnesium alloy and a 1 mm thick sheet of AA2024-T4 aluminium alloy. The dynamic tensile test properties of the AZ31B-H24 are taken from those reported in literature [8]. Material is seen to exhibit an average increase of 60-65 MPa with increased strain rate and also loss of 125 MPa in strength at 5% plastic strain at 250°C. Hence it has sufficient strain rate sensitivity and thermal softening effect. The modified Johnson-cook model with the Cowper-Symonds formulation (equation 1) is used for Mg-alloy and Johnson-cook model (equation 2) is used for Al-alloy.

$$\sigma = \left(A + B\varepsilon_p^n\right)\left[1 + \left[\frac{\dot{\varepsilon}}{C}\right]^{\frac{1}{p}}\right]\left[1 - \left(\frac{T - T_R}{T_M - T_R}\right)^m\right] \quad (1)$$

$$\sigma = \left(A + B\varepsilon_p^n\right)\left[1 + C\left[\frac{\dot{\varepsilon}}{\dot{\varepsilon}_0}\right]\right]\left[1 - \left(\frac{T - T_R}{T_M - T_R}\right)^m\right] \quad (2)$$

Where T, T_R, T_M are temperature studied, Room temperature & Melting temperature respectively.

The experimental data for Mg-alloy AZ31B fitted to above equation using non-linear regression technique by Hasenpouth [8] has been used, as tabulated below:

Parameter	Estimate	Lower 95%	Upper 95%
A [MPa]	202.768	190.136	215.400
B [MPa]	180.932	171.468	190.396
n	0.229	0.193	0.265
C [1/s]	5e4	-	-
p	2.157	2.109	2.205
m	1.393	1.380	1.406

Table 1: *Parameter in CS model for Mg AZ31B-H24 for rolling direction [8]*

The above fitted values have an R-Squared value of 0.97. Hence the model captures the behavior reasonably well. However, there are issues at very high strain rates. For AA2024-T4, parameters taken are as provided by Ouk Sub Lee [9].

A [MPa]	B [MPa]	N	C	m	$\dot{\varepsilon}_0[s^{-1}]$	$T_R[K]$	$T_M[K]$
390	1980	0.4890	0.0140	0.6	0.0001	298	775

Table 2: *Parameters in JC model for AA2024-T4 [9]*

At high temperature, different mechanical and electrical properties of the material also vary significantly. All these properties such as electrical conductivity, young's modulus, coefficient of thermal expansion [7, 10-12] at high temperature are considered.

3 Failure Criteria Based on Strain Distribution

As discussed by Hasenpouth [8], in simulations, the fitted material models were not able to predict the necking of the samples. So in the present study, a Thickness strain non-uniformity based failure criterion is introduced. Namely, the "Strain Non-uniformity Index" [13-15] is used to represent quality of strain distribution. This factor is the outcome of a combined effect of geometric, material and process parameters on the strain distribution. This is given by the difference between Peak thickness Strain and Average thickness strain of the formed part, computed at every time step. The corresponding curvature (K) of the strain peaks is also calculated as given by equation 3.

$$K = \left(\frac{d^2\varepsilon}{dx^2}\right) / \left[1 + \left(\frac{d\varepsilon}{dx}\right)^2\right]^{3/2} \tag{3}$$

This curvature in terms of the SNI is given by equation 4.

$$\frac{d^2\varepsilon}{dx^2} = SNI + \sum_{n=1}^{m} - \left[1 + \left(\frac{n\pi}{L}\right)^2\right]\left[a_n cos\left(\frac{n\pi x}{L}\right) + b_n sin\left(\frac{n\pi x}{L}\right)\right] \tag{4}$$

Where L is the length of the sheet for which strain distribution is considered, a_n & b_n are Fourier coefficients.

The derivation of the same will be given elsewhere [15]. High curvature value represents a sharp peak and the strain is more likely to localize there. This way, failure of a material can be pre-empted by this strain distribution based method. Hence, SNI combined with curvature of the peak completes a tool to predict the failure of the deforming sheet. The critical value of curvature at the strain peak and SNI can be determined from experiments.

To start with, thickness strain distribution data from the simulations is fitted into a Fourier series of appropriate order (about 850 in the present study). The R squared values obtained for the fits are all greater than 0.9970. Then Central difference numerical differentiation technique with 8th order accuracy was applied to obtain the curvature at the peaks. Here, many peaks may not be captured until enough numbers of data points are present to define a particular peak. Hence additional numbers of intermediate data points

were generated using Fourier fit. Accuracy is of prime concern and care was taken not to leave out strain peaks.

4 Design of Simulations

In the current study, cavity fill simulations of two metals have been carried out with two levels of temperatures and energy. Two different end constraint conditions posed affect the strain distribution thereby influencing the SNI and peak curvature values. To see the effect on cavity fill in various conditions, following factors and their levels have been chosen (Table 3).

Factor	**Level 1**	**Level 2**
Sheet End Constraint	Fully Free (FF)	Fully Constrained (FC)
Material	Mg alloy (AZ31B-H24)	Al alloy (AA2024-T4)
Energy Levels	4.3 kJ	8.2 kJ
Initial temp. of sheet	423K	523K

Table 3: *Factors and their respective levels*

Run	**Sheet End Constraint**	**Material**	**Energy Level (kJ)**	**Initial temp. of sheet (K)**	**SNI**	**H_F/H_T X 100**
1	FF	AZ31B	4.3	423	0.0156	34.64534
2	FF	AZ31B	4.3	523	0.0167	36.37234
3	FF	AZ31B	8.2	423	0.0299	43.20681
4	FF	AZ31B	8.2	523	0.0378	46.11756
5	FF	AA2024	4.3	423	0.0106	36.90238
6	FF	AA2024	4.3	523	0.0145	36.93281
7	FF	AA2024	8.2	423	0.0229	50.49213
8	FF	AA2024	8.2	523	0.0278	54.56981
9	FC	AZ31B	4.3	423	0.0129	29.25869
10	FC	AZ31B	4.3	523	0.0151	33.10647
11	FC	AZ31B	8.2	423	0.0259	35.53459
12	FC	AZ31B	8.2	523	0.0298	39.58488
13	FC	AA2024	4.3	423	0.0110	31.75159
14	FC	AA2024	4.3	523	0.0132	32.97294
15	FC	AA2024	8.2	423	0.0194	42.00009
16	FC	AA2024	8.2	523	0.0215	47.23350

Table 4: *Full factorial design of the selected factors with their respective levels & corresponding SNI and H_F/H_T values*

Two output parameters have been sought as the outcome of the simulations for analysis:

1. Strain non-uniformity Index (SNI)
2. Maximum filled groove height/Total groove height (H_F/H_T x 100)

Full factorial design of experiments is shown in Table 4. Analysis of Means (ANOM) approach [16] has been used to analyze the effect of these factors on the SNI and the degree of cavity filling. Aim here is to get maximum cavity fill without severe thinning or failure i.e. at low SNI.

5 Results and Discussion

Figures 3 and 4 show the main effect plots and interaction plots. Following Observations can be made:

1. Both materials show greater SNI for unclamped condition. However, SNI is less for Al-alloy as compared to Mg-alloy regardless of the status of clamping (figure 3b-1).
2. At higher discharge energy, end conditions also influence SNI significantly. Fully clamped condition shows smaller effect, while an unclamped condition shows a steeper increase in the SNI as seen from figure 3b-2.
3. Effect of temperature on the SNI is similar, regardless of the status of the clamping & material as seen from figure 3b-3 & 3b-5. However, Effect of temperature on SNI is pronounced when the discharge energy is high (figure 3b-6).
4. From the above it appears that low discharge energy, fully constrained condition and a low temperature favours a low SNI, as would be expected, also seen in Fig 3(a).

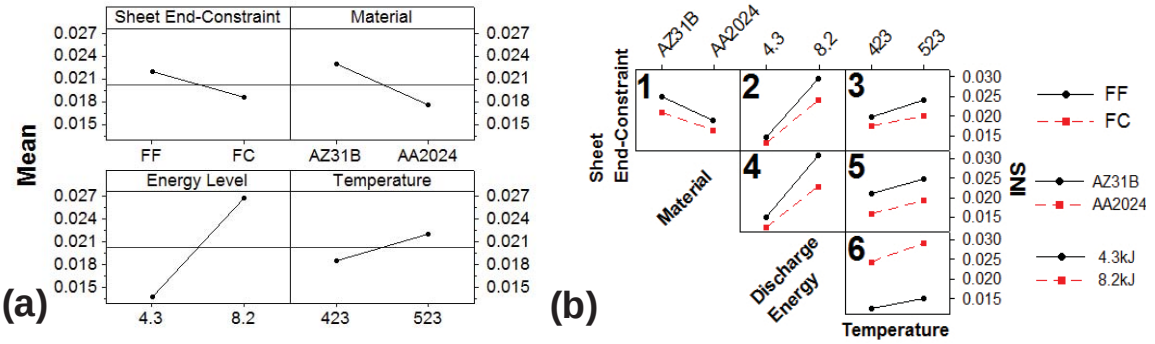

Figure 3: *(a) Main effect plots, (b) Interaction plots, of all the factors taking SNI as a response.*

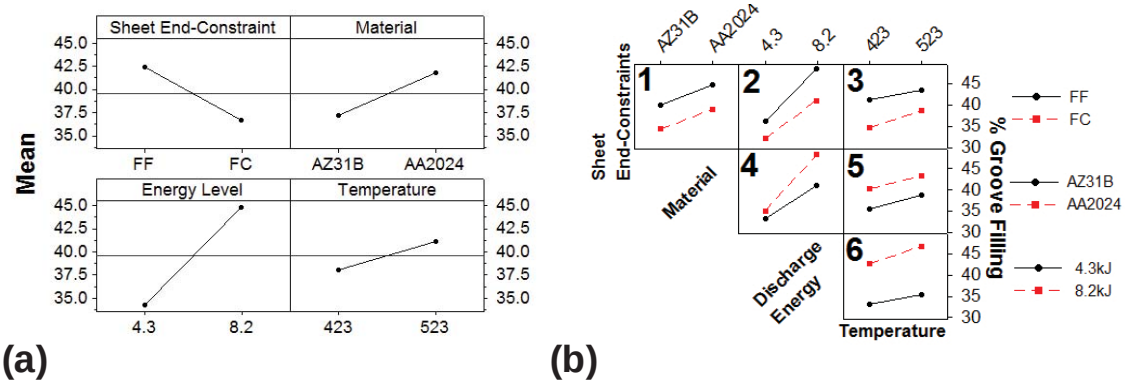

Figure 4: *(a) Main effect plots, (b) Interaction plots, of all the factors taking maximum filled groove height/Total groove height as a response.*

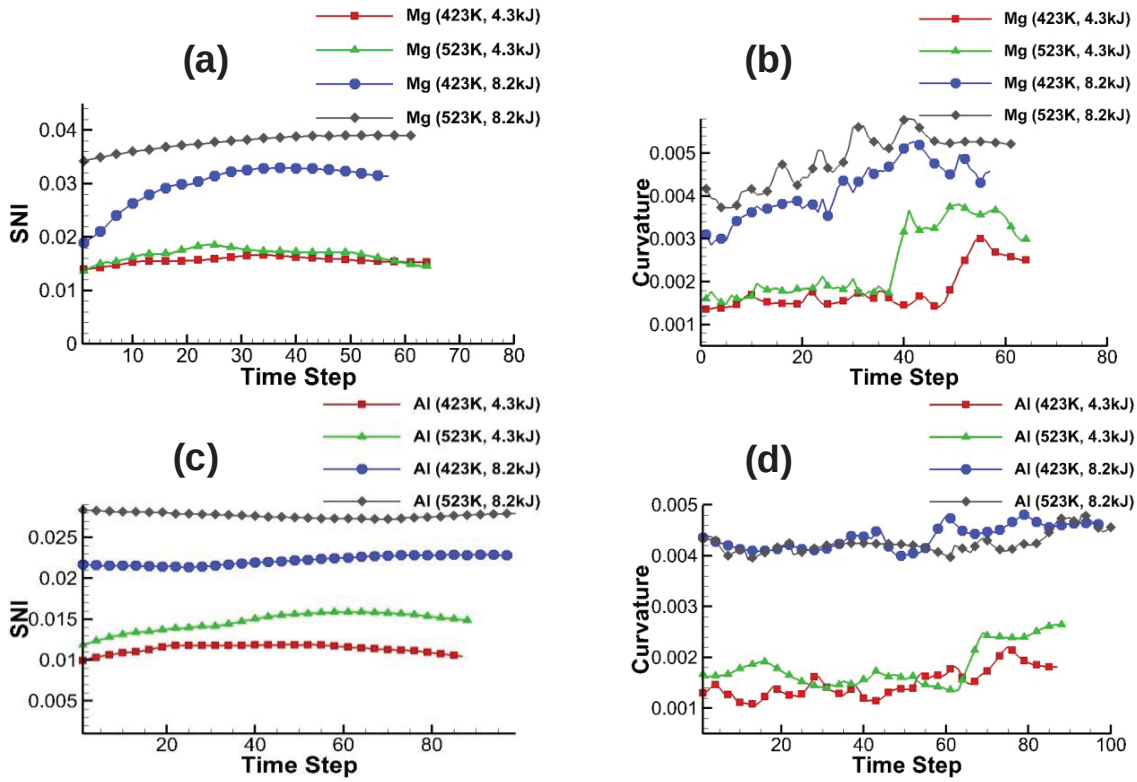

Figure 5: *(a) & (c) SNI plots, (b) & (d) Curvature plots for runs with Mg-alloy & Al-alloy respectively for fully free end condition.*

5. Filling is better with an unclamped condition. The cavity filling depth is equally sensitive to the status of clamping in case of the two materials. However, Aluminium shows higher depth of filling compared to Mg alloy irrespective of clamping conditions as seen from figure 4b-1.
6. With increasing discharge energy, increase in cavity filling is more rapid for an unclamped condition as seen from figure 4b-2.
7. Sheet in a fully clamped condition shows rapid die filling with increase in temperature. That is, die filling is more sensitive to temperature when the sheet is fully clamped (figure 4b-3).
8. With increase in discharge energy, groove filling in Al is far superior to that of Mg with smaller increase in strain non-uniformity (figure 3b-4 & 4b-4).
9. Cavity filling in Al improves at high temperatures particularly when energy is high, This improvement in deformation of Al with increase in temperature at high energy can be attributed to an inherently high electrical conductivity, decreasing flow strength with temperature and a relatively insignificant reduction in induced forces due to lower electrical conductivity at high temperatures.
10. Sensitivity of die filling to temperature increases with an increase in discharge energy. Die filling is better if temperature is increased. (figure 4b-6)
11. For better die filling, a high discharge energy, unclamped condition and high temperature are recommended. This is also confirmed by figure 4a.
12. From figures 5 & 6, conclusions emerge to be consistent with those from ANOM analysis discussed. Increase in SNI & Curvature values is very sensitive to increase in

discharge energy. Also with increased energy, the role of SNI seems to become increasingly significant (based on high ratios of SNI to curvature).

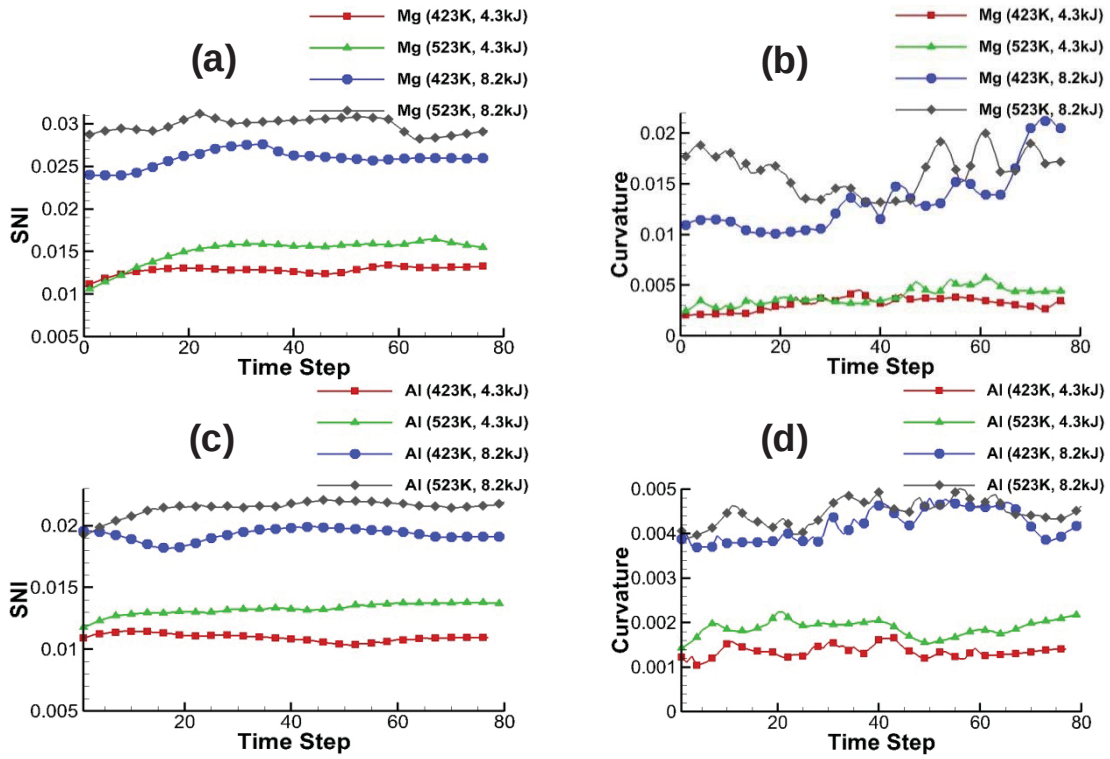

Figure 6: *(a) & (c) SNI plots, (b) & (d) Curvature plots for runs with Mg-alloy & Al-alloy respectively for fully constrained end condition*

13. Al shows lower curvature at the peak, which is far more sensitive to discharge energy than to temperature within the range of temperatures studied. SNI does increase with increasing temperature. Inferences drawn from Fig. 5 & 6 hold irrespective of clamping conditions.
14. The variation in curvature values arises out of continuous shifting of peak curvature point. Sheet tends to localize near the first cavity for clamped case and near the third cavity for unclamped case.

6 Conclusions

1. Low discharge energy, fully constrained condition and a low temperature favours a low SNI whereas for better die filling, a high discharge energy, unclamped condition and high temperature are recommended. It is therefore seen that the favourable conditions for die filling and a more uniform strain distribution counter each other.
2. Optimum conditions permitting some degree of drawing in, together with optimal discharge energy could be established at a given temperature of forming to facilitate rapid die filling at a low SNI.
3. Regulated blank holding force could be a better alternative as it includes advantages

of both clamped (uniformity in filling) & unclamped (higher depth of filling).

4. Effect of decrease in deformation with increased temperature becomes more and more immaterial if discharge energy used is near upper bound value of discharge energy to form a sample at the given temperature without failure.
5. The critical value of SNI and curvature may be verified experimentally.

References

[1] Luo, A.: Magnesium: current and potential automotive applications. JOM 2002, v.54, p.42-48.

[2] Watarai, H.: Trends of Research and Development for Magnesium Alloys – Reducing the Weight of Structural Materials in Motor Vehicles. Science and Technology Trends, Quarterly Review, No. 18, 2006, p.84-97.

[3] Wu, H. Y., Lin, F. Z.: Mechanical properties and strain-hardening behavior of Mg alloy AZ31B-H24 thin sheet. Materials Science and Engineering A, v.527(4-5), 2010, p.1194-1199.

[4] Ulacia, I., Arroyo, A., Eguia, I., Hurtado, I., Gutierrez, M. A.: Warm Electromagnetic Forming of AZ31B Magnesium Alloy Sheet. In: Proc. of 4th Int. Conf. High Speed Forming, 2010, p.159-168.

[5] Murakoshi, Y., Katoh, M., Matsuzaki, K., Saigo, M.: High Velocity sheet bulge forming of magnesium alloy by electromagnetic forming. In: Proc. 9th Int. Conf. Tech. Plasticity, 2008, p.1010-1015.

[6] Ulacia, I., Imbert, J., Salisbury, C. P., Arroyo, A., Hurtado, I., Worswick, M. J.: Electromagnetic Forming of AZ31B Magnesium Alloy Sheet : Experimental Work and Numerical Simulation, In: Proc. of 3rd Int. Conf. High Speed Forming, 2008, p.191-200.

[7] COMSOL Multiphysics User's Guide, 2011.

[8] Hasenpouth, D.: Tensile High Strength Behavior of AZ31B Magnesium alloy Sheet, M.S. Thesis, University of Waterloo, Canada, 2010.

[9] Lee, O. S., Choi, H., Kim, H.: High-temperature dynamic deformation of aluminum alloys using SHPB. Journal of Mechanical Science and Technology, v.25(1), 2010, p.143-148.

[10] Military Handbook-5H, Metallic Materials and Elements for Aerospace Vehicle Structures. Dec. 1998, p.3-68.

[11] Busk, R.S.: Magnesium and its alloys, Magnesium Products Design, Pub. Marcel Dekker, Inc., 1987.

[12] Lalpoor, M., Eskin, D. G., Katgerman, L.: Cold-cracking assessment in AA7050 billets during DC-casting by thermo-mechanical simulation of residual thermal stresses and application of fracture mechanics. Metall. Mater. Trans. A, 40(13), 2009, p.3304–33.

[13] Desai, S., Date, P.: On the quantification of strain distribution in drawn sheet metal products. Journal of Materials Processing Technology, v.177(1-3), 2006, p.439-443.

[14] Date, P. P., Desai, S. G.: Strain distribution based formability criteria in sheet metal forming of drawn automotive components, Symposium on Automotive Sheet Metal Forming, (Ed : D. Bhattacharjee), Tata Steel, Jamshedpur, India, 2007.

[15] Date, P. P.: Unpublished work, 2012.

[16] Montgomery, D. C.: Design and Analysis of Experiments, Pub. John Wiley & Sons, Inc. 1997.